Quantitative phenological observations of a mixed beech forest in northern Switzerland with digital photography

Hella Ellen Ahrends[1]; Robert Brügger[1]; Reto Stöckli[2,3]; Jürg Schenk[1]; Pavel Michna[1]; Francois Jeanneret[1]; Heinz Wanner[1]; Werner Eugster[4]

[1] Institute of Geography, University of Bern, Hallerstrasse 12, CH-3012 Bern, Switzerland

[2] Federal Office of Meteorology and Climatology MeteoSwiss, Climate Services, Climate Analysis, Krähbühlstrasse 58, CH-8044 Zürich, Switzerland

[3] Department of Atmospheric Science, Colorado State University, Fort Collins, CO 80523, USA

[4] Institute of Plant Sciences, ETH Zürich, Universitätsstrasse 2, CH-8092 Zürich, Switzerland

corresponding author:

Hella Ellen Ahrends

University of Bern, Institute of Geography

Hallerstrasse 12

CH-3012 Bern

Tel.: +41(0)446327981

Fax: +41(0)446321153

ahrends@giub.unibe.ch

Abstract

Vegetation phenology has a strong influence on the timing and phase of global terrestrial carbon and water exchanges and is an important indicator of climate change and variability. In this study we tested the application of inexpensive digital visible-light cameras in monitoring phenology. A standard digital camera was mounted on a 45 m tall flux tower at the Lägeren FLUXNET/ CarboEuropeIP site (Switzerland), providing hourly images of a mixed beech forest. Image analysis was conducted separately on a set of regions of interest representing two different tree species during spring in 2005 and 2006. We estimated the date of leaf emergence based on the levels of the extracted red, green and blue colors. Comparisons with validation data were in accordance with the phenology of the observed trees. The mean error of observed leaf unfolding dates compared with validation data was 3 days in 2005 and 3.6 days in 2006. An uncertainty analysis was performed and demonstrated moderate impacts on color values of changing illumination conditions due to clouds and illumination angles. We conclude that digital visible-light cameras could provide inexpensive, spatially representative and objective information with the required temporal resolution for phenological studies.

Introduction

Phenology is the study of recurring biological events in the biosphere and the causes of their timing [*Lieth*, 1976]. Historically, phenological studies have been performed in agriculture to document events such as plant emergence, fruiting and harvest. In recent decades phenology has become recognized as an important integrative method for assessing the impact of climate variability and climate change on ecosystems

[*Menzel*, 2002; *Sparks and Menzel*, 2002]. Recent global warming has had significant effects on the seasonality of ecosystems [*Badeck et al.*, 2004; *Chuine et al.*, 2004; *Peñuelas and Filella*, 2001; *Zhang et al.*, 2007]. Time series analyses of selected variables such as green-up, maturity, senescence and dormancy, yield valuable information about ecosystem responses to climate and are widely used in climatological and ecological models [*Cleland et al.*, 2007; *Reed et al.*, 1994; *Schwartz*, 1994]. Plant phenology is strongly connected to the gas and water exchange of ecosystems [*Davis et al.*, 2003; *Knohl et al.*, 2003; *Moore et al.*, 1996]. Shifts in phenology can therefore significantly affect the global carbon and water cycle [*Baldocchi et al.*, 2005; *Churkina et al.*, 2005; *Piao et al.*, 2007]. Consequently, a knowledge and understanding of these phenological processes is needed for the parameterization of models used in climate predictions [*Arora and Boer* 2005; *Lawrence and Slingo*, 2004a, 2004b; *Lu et al.*, 2001].

Phenological ground observations span several decades, sometimes up to centuries [*Rutishauser et al.*, 2007], but they are often observer-biased [*Kharin*, 1976; *Menzel*, 2002]. Additionally, there is a significant decline in long-term observation sites due to a lack of volunteers for phenological field work. For two decades satellite remote sensing has been providing a globally integrated view of vegetation phenological states. However, this method still heavily depends on ground-based measurements for validation. Moreover, satellite images often have limited temporal and spatial coverage due to clouds, aerosols and other atmospheric- or sensor-related characteristics [e.g., *Ahl et al.*, 2006; *Fisher et al.*, 2006; *Studer et al.*, 2007; *Zhang et al.*, 2004, 2006]. Within the framework of the COST Action 725 ("Establishing a European Phenological Data Platform for Climatological Applications"), our project investigates the application of

47 ground-based, commercially available digital cameras in observational procedures and
48 quality assurance of phenological monitoring.

49 Overall, the adoption of standard digital visible-light cameras in ecological research
50 has been slow but recently an increasing number of studies have used digital images from
51 standard ground-based RGB (red, green and blue) cameras for vegetation studies. In an
52 early approach *Brandhorst and Pinkhof* [1934] compared flowering and leaf development
53 of common park trees with dated analog photography, and emphasised the use of
54 photography for objective phenological monitoring. Vertical sky-ward wide-angle
55 photography has been successfully used for monitoring changing light conditions in
56 forests, Leaf Area Index (LAI) and canopy-closure-estimation [*Rich*, 1988, 1990; *Rich et*
57 *al.*, 1993]. This technique was first used for forests by *Evans and Coombe* [1959] and is
58 currently widely applied [*Jonckheere et al.*, 2004; *Nobis and Hunziker*, 2005; *Pellika*,
59 2001]. Vertical downward photography for the quantification of parameters such as
60 vegetation fraction, LAI and biomass was performed by *Vanamburg et al.* [2006], *Zhou*
61 *et al.* [1998, 2001] and *Behrens and Diepenbrock* [2006]. Other approaches analyzed
62 vertical vegetation structures [*Zehm et al*., 2003] and directional reflectance distributions
63 of vegetation targets [*Dymond and Trotter*, 1997] with multiple digital images. The link
64 between leaf pigmentation and digital images was found by *Kawashima and Nakatani*
65 [1998] who estimated the chlorophyll content in leaves using a video camera. Net CO_2
66 uptake of moss was analysed by *Graham et al.* [2006] with a RGB camera based upon the
67 changes in reflected visible light (VIS) during moss drying and hydrating. The
68 observation of phenological phases was first tested by *Adamsen et al.* [1999], who
69 analysed wheat senescence with a digital camera. *Sparks et al.* [2006] used monthly

fixed-date, fixed-subject photographs to examine the correlation between plant phenology and mean monthly meteorological data. Digital camera images, phenology and satellite-based data were jointly analyzed by *Fisher et al.* [2006], who used multiple photographs, visually classified by independent observers, as validation data for satellite model estimates of phenological development. The latest research in webcam-based phenological monitoring was published by *Richardson et al.* [2007]. Digital webcam-images were successfully used for spring green-up tracking of a forest and jointly analyzed with FAPAR (fraction of incident photosynthetically active radiation absorbed by the canopy), broadband Normalized Difference Vegetation Index (NDVI) and the light-saturated rate of canopy photosynthesis, inferred from eddy covariance measurements at a flux tower site.

Despite this pioneering work, the application of digital image analysis in vegetation phenology is still a young field. Previous studies mainly documented the conceptual use of area-integrated digital camera images in vegetation monitoring. Spatial and temporal uncertainty of digital images for continuous objective monitoring of phenological processes is still largely unknown. Species-specific image analysis, comparable with traditional phenological observations in a mixed forest canopy, has not yet been conducted. In this study we conducted species-specific phenological observation using digital photography, incorporating an uncertainty analysis, for a managed mixed forest in northern Switzerland. We focussed on the forest spring phenology in 2005 and 2006, and aimed to identify leaf unfolding dates of the two dominant tree species, beech (*Fagus sylvatica* L.) and ash (*Fraxinus excelsior* L.). The automated observation of different species presented in our study here adds a further level of complexity and requires the

93 separation of the phenological signal of single species from that of their surroundings.
94 Given that within a mixed canopy the phenology of individual trees is locally adapted to
95 environmental conditions such as light or tree age [e.g., *Kikuzawa*, 2003] we observed
96 three ash and two beech trees using the camera. Additionally, we observed spring green-
97 up of a mixed forested region located a few kilometers from the camera. Extending the
98 work of previous studies, we conducted an uncertainty analysis, a species-dependant
99 phenological observation including a year-to-year comparison, and interpreted the camera
100 signal in detail. We were therefore able to examine both the potential and the limitations
101 of this novel observation method.
102
103 **Materials and Methods**
104 *Site description*
105 The Lägeren research site is located at 47°28'49''N and 8°21'05''E at 682 m a.s.l.
106 on the south slope of the Lägeren mountain, approximately 15 km northwest of Zürich,
107 Switzerland. The south slope of the Lägeren mountain marks the boundary of the Swiss
108 Plateau, which is bordered by the Jura and the Alps. Since 1986 the Lägeren site has been
109 a permanent station of the Swiss air quality monitoring network (NABEL) [*Burkard et*
110 *al.*, 2003]. A 45 m tall flux tower provides micrometeorological data at a high temporal
111 resolution. Routine CO_2 and H_2O flux measurements as a contribution to the FLUXNET/
112 CarboEuropeIP network started in April 2004 [*Eugster et al.*, 2007]. The mean annual
113 temperature is 8°C. The mean annual precipitation is 1200 mm and the vegetation period
114 is 170-190 days. The natural vegetation cover around the tower is a mixed beech forest.
115 The western part is dominated by broad-leaved trees, mainly beech (*Fagus sylvatica* L.)

and ash (*Fraxinus excelsior* L.). In the eastern part beech and Norway spruce (*Picea abies* (L.) Karst.) are dominant. The forest stand has a relatively high diversity of species, ages, and diameters [*Eugster et al.*, 2007].

The vegetation cover within the camera's field of view predominantly consisted of beech, ash and silver fir (*Abies alba* Mill.). Understory vegetation varies, but during the study period it was dominated by bear garlic (*Allium ursinum* L.) and beech saplings.

Technical set-up

On the uppermost platform of the Lägeren flux tower a standard digital 5-megapixel camera (NIKON Coolpix 5400, CCD sensor) was connected to a Linux-based computer and mounted in a weatherproof enclosure. The camera provides hourly digital raw images (2592x1944 pixels, 12 bit color resolution) of the Lägeren forest since autumn 2004. This camera was chosen because of its high sensor resolution, good quality optics and its ability to store images in uncompressed raw format. Quantitative image analysis requires the original and complete image information. Spatial or color compression (e.g. JPEG) by the camera's complex and proprietary image processing algorithms can potentially lead to information loss and nonlinearities [*Stevens et al.*, 2007]. Raw files contain the actual pixel data captured by the camera sensor, before it has undergone any processing method. Furthermore, in the raw format, information such as white balance, saturation, color space or tonality are included as metadata and can be adjusted manually by the user following image capture. The field of view of the camera is approximately 60° wide and the view angle is tilted 25° below the horizon. A sample image is presented in Figure 1.

Image capture was controlled by custom Perl (Practical Extraction and Report Language) scripts and the open-Source software gphoto2 (http://gphoto.org). To cope with diurnally and seasonally changing illumination conditions the camera was operated in the automatic exposure and aperture mode. The camera was pointed towards the west, looking at the southern slope of the Lägeren mountain. The sun therefore moved from behind to in front of the camera over the course of a day.

As shown in Figure 1 a color calibration panel was included in the camera's field of view, but was not in the image analysis since reflection values were saturated on sunny days.

Image analysis

The NIKON raw image format (NEF) was processed into standard TIFF (Tagged Image File Format) without performing white balance, changes in color space, and without applying any automatic correction methods or filters, maintaining the original image information. The TIFF images (linearly scaled to 48 bit color resolution) provided a time series of digital data in the visible part of the electromagnetic spectrum (located approximately between 400 – 700nm), at an hourly temporal resolution (excluding the dark hours). This scheduling was chosen so as to provide an adequate temporal resolution under limited data storage capacity.

Data analysis was based on 64 midday images for 2005 and 67 images for 2006 between Day of Year (DOY) 101 (April 11) and 170 (June 19). Only the images taken near local noon time were used in order to minimize angular effects of the forest canopy's hemispherical directional reflectance function (HDRF) [*Chen et al.*, 2000]. This selection

was supported by an uncertainty analysis examining the influence of diurnal illumination changes on camera-based phenology. Images with raindrops on the camera lens, images of very foggy days or days with snow cover were excluded from the time series analysis. Image analysis was conducted separately on each region in a set of regions of interest (ROIs) representing single tree species (Figure 1). Each ROI covered a specific set of species, and within each of these there was variation in vegetation during spring due to changing leaf coverage: closer trees masked those further away during green-up. As an extension to previous studies our analysis here explores the effects of these overlaying signals. Table 1 shows the different species included within the different ROIs. Regions of interest were named after the dominant tree species. We observed the phenology of three ash and two beech trees. The Beech 2 ROI and the Beech 3 ROI were mainly covered by the same tree, Beech 2 representing its upper crown and Beech 3 representing the lower crown and part of the understory vegetation. Beech trees generally show successive leafing, starting at the lower parts of the crown and moving up to the top of the crown [e.g., *Kikuzawa*, 1983; *Kikuzawa*, 1989; *Kikuzawa*, 2003]. Therefore we compared leafing dates of the Beech 2 ROI with those from the Beech 3 ROI. The Background Forest ROI was chosen in order to measure spatially integrated phenology characteristics of a heterogeneous area and to study the atmospheric disturbance effects at a larger distance from the camera.

The image's color values (red, green and blue) were extracted and averaged across each ROI at daily intervals. Several vegetation indices have been developed to describe biomass amount and vegetation status. Since the camera's spectral sensitivity is limited to the visible part of the spectrum, we used the relative brightness of the green channel (GF:

185 the ratio of the mean raw green value to the sum of the mean raw red, green and blue
186 values):

187 $$GF = (G / (G+R+B))$$

188 The exact spectral sensitivity of the NIKON Coolpix 5400 was not revealed by the
189 manufacturer. The GF was computed from unsmoothed and non-interpolated mean color
190 values for each ROI and was a suitable index for recording changes in vegetation state
191 during spring. GF values were then plotted over time to describe changing phenology in
192 the observed ROIs (Figure 2). Leaf emergence dates were (a) automatically determined
193 using first and second derivatives ($\Delta GF/\Delta t$ and $\Delta^2 GF/\Delta t^2$) describing curvature changes
194 (data not shown) and (b) by visual curvature shape interpretation. Generally leaf
195 emergence is represented by the maximum value of the second derivative, that is, by the
196 starting date of a significant GF increase (inflection point). The derivative methodology is
197 very responsive to noise in the unsmoothed GF time series. It was successfully applied to
198 Beech 1, 2 and 3, Background and Ash 3 ROIs. For the Ash 1 and 2 ROIs, leaf
199 emergence dates were derived visually from the GF curvature shape as there was
200 interference in the data from the earlier greening of background vegetation and
201 understory (see in the following section).

202 Validation data were obtained from daily visual image interpretation combined with
203 direct phenological observations of sample trees performed by the Forestry Office
204 Wettingen. In 2006 the percentage of foliation in the upper, middle and lower part of Ash
205 3 and Beeches 1, 2 and 3 was documented between DOY 115 (25 April 2006) and 124 (4
206 May 2006) (data not shown). Leaf unfolding dates for the Ash 1 and 2 ROIs were
207 visually estimated from imagery (Table 2). In 2005 validation data for all ROIs was

visually estimated. Comparisons of field observations from 2006 with 2006 imagery served as reference. The human eye is readily able to differentiate between different stages of leaf emergence justifying visual image interpretation ("visual leaf unfolding" in Table 2). Visual interpretation of Background forest phenology further resulted in a higher uncertainty.

Uncertainty analysis

Pixel values and therefore GF values and leaf emergence dates are influenced by different biotic and abiotic factors. Uncertainties and variations on daily and hourly time-scales are thought to be mainly a result of abiotic factors such as changing ambient illumination conditions and wind influences.

It can be assumed that the tree positions in the images changed due to tower and tree movements on windy days. Wind influences and natural leaf development led to different leaf inclination angles which may have influenced the levels of the extracted color values. We did not consider these influences within this study. To quantify uncertainties we focussed on ambient illumination conditions. They affect results because of (a) changing radiation due to clouds and humidity, (b) diurnally and seasonally changing illumination angle, and (c) the limited dynamic range of the camera. Due to clouds and other atmospheric influences, such as water vapour content, the fraction of direct radiation changes over time. Its impact on photosynthetic activity and surface albedo was described e.g. by *Wang et al.* [2002], *Rocha et al.* [2004] and *Gamon et al.* [2006]. Also, dependencies of vegetation index values on illumination angles are well known [*Holben*, 1986]. Amongst others, *Holben and Kimes* [1986], *Jackson et al.* [1990]

231 and *Schaaf and Strahler* [1994] have shown that surface anisotropic properties have a
232 significant influence on surface reflectance measurements. The effect of the illumination
233 angle is dependent on vegetation type, varies with spectral wavelength and is difficult to
234 quantify [*Qi et al.*, 1995]. Using sample images we analyzed the variance due to both
235 cloud conditions and to changing illumination angles, and quantified the impacts on the
236 GF.

237 We attempted to quantify the impact of changing fractions of diffuse radiation on
238 the GF by comparing vegetation indices of (visually classified) "cloudy" and "sunny"
239 images. We compared eight pairs of sunny and cloudy images from successive days taken
240 at midday in the middle and at the end of the growing season. Except for the radiation,
241 stable environmental conditions were assumed for the picture pairs. GF values of the
242 images with higher diffuse radiation fractions ("cloudy" days: DOY 144, 155, 163, 168,
243 209, 229, 234 in 2005) were subtracted from those with high direct radiation fraction
244 ("sunny" days: DOY 145, 154, 162, 167, 169, 208, 228, 235 in 2005). For each ROI and
245 each pair of images the relative change of the GF was calculated (values normalized with
246 the GF of the "sunny" images):

247

248 $$\Delta GF\ [\%] = (1 - GF_{cloudy} / GF_{sunny}) * 100\ [\%]$$

249

250 Moreover, we hypothesized that changing diurnal illumination angles could have a
251 significant impact on image pixel values and thus also on the GF. To test this assumption
252 we calculated GF variation over five sunny days in the middle and at the end of the
253 growing season of 2006 (DOY 163, 175, 181, 198 and 211). Mean RGB values were
254 extracted from hourly digital images between 7:30 and 15:30 hours.

255

256 **Results**

257 *Temporal spectral response of the GF*

258 Figure 2 shows the GF curves and GF-derived leaf emergence dates for 2005 and
259 2006. The GF showed a characteristic curve shape, similar to spring leaf emergence
260 phenology, and could therefore be used as a surrogate index for phenological phases.
261 Generally the values showed species-specific seasonality. Short-term variations (noise
262 component) were similar for each ROI.

263 The Ash 1 ROI and the Ash 2 ROI displayed two consecutive pronounced rises in
264 spring. The first rise was due to the leaf emergence of trees or understory vegetation in
265 the background with earlier green-up dates, whereas the second increase was caused by
266 the leaf flush of the ash. Figure 4 shows enlarged image data as an example of the Ash 2
267 ROI in spring 2006. This ROI was strongly influenced by a beech growing behind the
268 ash, having an earlier leaf emergence which was partially visible in the space between the
269 stem and bare branches of the ash tree in the foreground.

270 Figure 3 shows the red and blue color values normalized to the overall brightness
271 (red and blue fraction) for the ROIs Beech 1 and Ash 1 in 2005. The values were similar
272 in 2006 (data not shown). For both species, the blue fraction (BF) decreased
273 simultaneously with the increase of the GF during green-up while the red fraction (RF)
274 remained approximately constant.

275 After complete leaf expansion, when leaves were getting thicker, drier and darker
276 and reached their delayed full photosynthetic activity [e.g., *Morecroft et al.*, 2003;

277 *Schulze*, 1970], GF decreased in all ROIs, particularly in 2006. BF slightly increases and
278 the RF decreases at that time.

279 In 2006 the GF was generally lower than it had been in 2005. RF and BF values of
280 the Background Forest ROI were highly scattered but curve characteristics were similar
281 to the beech dominated ROIs (data not shown). Moreover, the Background Forest
282 reflection values were higher than those of the regions next to the tower (data not shown).
283 Since the camera adjusted exposure and aperture automatically, the background generally
284 appeared brighter than the foreground, especially with high diffuse radiation fractions. At
285 increasing distances from the camera higher atmospheric absorption and scattering of
286 light occurs [*Janeiro et al*., 2006]. Therefore the GF of the Background Forest ROI
287 showed a less consistent curve compared to the other ROIs.

288

289 *Validation of the GF*

290 Dates for the leaf emergence of the dominant tree species generally agreed well
291 with validation data (Table 2). ROIs with similar dominant tree species showed similar
292 GF curve shapes. GF curves in 2005 were more consistent than in 2006 (Figure 2). The
293 estimation of transition dates in 2006 was more difficult due to irregularities in the GF
294 curve. The mean error of observed onset compared with the validation data was 3 days in
295 2005 and 3.6 days in 2006. The maximum disagreement between validation and GF-
296 based estimates was eight days in 2005 and seven days in 2006 for the Ash 2 ROI. GF-
297 based dates for leaf unfolding for the beech-dominated ROIs showed better agreement
298 with validation data than the ash-dominated ROIs. Because of missing images between
299 DOY 116 and 119 in 2005 caused by a technical system failure, the derivation of the

300 exact date for beech leaf unfolding was not possible. This does not affect the general
301 finding that in both years the GF values in beech-dominated ROIs increased slightly
302 earlier than indicated by the validation data. Possibly, this demonstrates the high
303 objectivity and accuracy of the imagery for the observation of the budbreak. In field
304 studies it was difficult to observe the exact date for first leaf appearance. However, the
305 GF values may additionally be influenced by early leaf unfolding of beech saplings in the
306 understory vegetation. In contrast, GF values for ash-dominated ROIs increased after leaf
307 unfolding was observed in the field. As noted above, GF already increased for the ash-
308 dominated ROIs when other vegetation components such as the understory or beech trees
309 were greening up. Therefore, after leaf emergence of the ash tree, the GF values only
310 increased when ash leaves started covering branches, stem and other previously non-
311 green parts in the ROI. This is also the most likely cause for the greater disagreement
312 between the ash-dominated regions with the validation data.

313 The mean date of leaf unfolding was five days earlier in 2006 than in 2005 for
314 beech-dominated ROIs and six days earlier for ash-dominated ROIs. For the Background
315 Forest ROI leaf emergence started two days earlier in 2006. Maximum GF values of the
316 observed ROIs were reached between the middle and the end of May in both years.
317 Within species, the GF-based dates for the start of the growing season dates were very
318 similar. The delayed green-up of the Ash 1 ROI and the earlier green-up of the Ash 3
319 ROI in 2005 agreed well with validation data. In 2006 leaf emergence in the lower crown
320 layers, represented by the Beech 2 ROI, happened earlier than in the upper crown layers,
321 represented by the Beech 3 ROI. In 2005 this difference between the Beech 2 and the

Beech 3 ROIs did not show up in the GF values, probably because of the missing images between DOY 116 and 119.

Uncertainty Analysis

To quantify the impact of the diffuse radiation fraction on the GF values we compared eight pairs of sunny and cloudy images. Resulting mean and maximum estimated GF changes for each ROI are given in Table 3. As the chosen images do not represent extremely contrasting sky conditions, the values represent average uncertainty rather than maximum uncertainty. The impact was highest for the furthest ROIs, such as the Background Forest and Ash 1. Their greater distances from the camera made these parts of the images more susceptible to the effects of water vapour absorption and scattering processes (particularly on cloudy days with higher air humidity). Therefore, these parts generally appeared brighter, resulting in a higher impact on the GF. Also, the spatial variability caused by stronger contrasts between shadowed and sunny areas seemed to be compensated by the averaging of color values over the observed ROIs.

To test the impact of changing illumination angles we calculated the diurnal course of GF values over five sunny days of 2006 between 7:30 and 15:30 hours (Figure 5). Generally, GF values first increased and then decreased again. Maximum GF values were reached before midday, except for the Beech 3 ROI (Figure 5b). To quantify the impact the coefficient of variation (in percent) was calculated for each ROI. Largest variations were found in the Beech 3 ROI (Table 4). This ROI was significantly affected by shadow effects. All ROIs showed significant dependencies on the illumination angle. This supports our choice of using only noontime images. The computed values displayed, not

345 only effects of daily changes in illumination angles, but also revealed an effect of the
346 seasonal shift in the sun's position. For ash-dominated ROIs and the Background Forest
347 ROI GF values generally decreased from June to July. Beech-dominated ROIs showed
348 first a decrease between DOY 163 and 175, and afterwards remained constant.
349 Furthermore, varying radiation values, leaf inclination angles and environmental
350 conditions were influencing the result. GF values were generally more sensitive to
351 illumination angles than to variations in the diffuse radiation fraction.
352
353 **Discussion**
354 The image-based estimates of leaf emergence dates suggest that camera-based
355 observation of a forest-canopy provides temporally accurate and objective phenological
356 information at the species level.
357 In this study, we focused on the estimation of the leaf flushing date of two
358 deciduous tree species. Image data provides a variety of information about vegetation
359 development. However, without knowing the spectral sensitivity of the camera's sensor,
360 image color values do not allow us to draw firm conclusions with respect to
361 biogeochemical processes such as photosynthetic efficiency [*Kira and Kumura*, 1983].
362 Nevertheless, the GF was found to be a reliable measure for the timing of biophysical
363 processes such as leaf emergence and expansion in spring. Maximum GF values represent
364 vegetation cover fraction and maximum canopy closure within the ROI. Therefore the GF
365 allows, within a specific uncertainty due to mixed species, objective statements about
366 phenology and leaf emergence rates. These estimates can be compared with data obtained
367 by ground-based field studies. Moreover the GF describes optical leaf color such as leaf

368 darkening due to chlorophyll accumulation [e.g., *Bray and Sanger*, 1961; *Bray et al*.,
369 1966] and changes in the leaf surface due to maturity and aging processes [e.g., *Ito et al*.,
370 2006]. However, the decrease in the GF after complete leaf expansion which was
371 observable in all ROIs may have been additionally influenced by seasonal changes of
372 midday sun angles as described in our uncertainty analysis.

373 Due to the mixed background signal from the variety of species, GF values did not
374 provide a method for estimating the leaf area index [*Chen and Black*, 1992] for the ROIs.
375 We found a generally lower green fraction in 2006. Field studies showed that 2006 was a
376 mast year for the beech and possibly the ash. Fruiting beech trees generally have more
377 transparent crowns because a proportion of the buds have developed into flowers and the
378 leaf size is reduced [*Innes*, 1994]. This could be a possible explanation for the lower GF
379 levels in these ROIs. However, observed similarity of short-term GF variations
380 demonstrate the larger influence of environmental conditions, e.g. illumination
381 conditions. Therefore, it is also reasonable that the lower GF values were caused by
382 abiotic factors.

383 Not only species-specific but also individual leaf unfolding dates could be
384 observed. Individual trees experience different green-up dates due to genetic differences
385 and based on their position within the forest canopy. The GF-based leaf unfolding date
386 was up to one week later for the Ash 1 ROI in 2005 compared to the other ash-dominated
387 ROIs. This ROI was mainly covered by a relatively free-standing ash tree compared with
388 the other ash trees within the camera's field of view. Although the delayed leaf unfolding
389 could not be shown with GF values for 2006, the observation is consistent with the
390 validation data. Our results agree with studies from *Brügger et al*. [2003] about the

391 phenological variability within one species due to the genetic differences and the
392 different social positions of the individual trees. Successive leafing processes moving
393 from lower to upper parts of the foliage could be observed for beeches during field work
394 but only showed up in the image data for 2006. The mean error for the estimation of the
395 leaf unfolding dates was larger than the variation in the leaf unfolding dates for the
396 different parts of the crown.

397 Our study also found less consistent GF curves for the Background Forest ROI
398 located a few kilometers from the camera compared to the other ROIs which were next to
399 the tower. The higher noise component of the GF for this ROI made an automated
400 detection of phenological transition dates much more difficult. However, since the
401 Background Forest ROI covers a set of different tree species, GF values probably
402 represent the maximum time span of leaf development for the sampled trees.

403 The GF is strongly influenced by the different species included within the ROIs.
404 Therefore the installation of phenological cameras should be performed cautiously with
405 respect to the different species included in the cameras field of view. An observation with
406 camera images of the understory green-up provides useful additional information. For
407 instance, since the phenological studies with satellite images based on the NDVI [e.g.,
408 *Tucker*, 1979] are strongly influenced by the earlier green-up of understory and saplings,
409 analyses of the image's color values can be used for objective satellite data validation.
410 However, comparisons with satellite data should be performed with respect to the timing
411 of phenological processes rather than as a quantitative comparison. For a realistic
412 validation and for the comparison of imagery from different cameras the spectral
413 calibration of the camera model under use would be required [*Stevens et al*., 2007].

In recent years eddy covariance measurements have been performed worldwide at flux tower sites for calculating local and regional carbon dioxide and water balances. In this context, shifts in phenology could significantly affect annual carbon uptake and water cycling [i.e., *Baldocchi et al*., 2005; *Churkina et al*., 2005; *Gu et al*., 2003; *Keeling et al.*, 1996; *Morecroft et al.*, 2003; *Niemand et al.*, 2005; *Piao et al.*, 2007; *White et al.*, 1999]. Therefore *Baldocchi et al.* [2005] suggested installing video cameras at flux tower sites for continuous monitoring of the canopy state. Since photographic cameras have a much better image resolution and quality than video cameras, our study suggests that still digital cameras may be better suited for this purpose. However, since measurements of the net ecosystem carbon dioxide exchange are strongly related to leaf gas exchange and therefore to photosynthetic activity and biomass, comparisons with GF values from standard digital images should also be based on the timing of phenological phases rather than on quantitative data. We believe that the installation of digital cameras can be used to bridge the gap between CO_2 flux measurements at ecosystem scale and satellite-based vegetation monitoring at a regional scale. Continuous time series of digital images of the forest canopy could complement terrestrial monitoring of gas and water exchanges at forest sites.

We found a considerable sensitivity of the GF to illumination conditions, mainly to changing sun angles. The interpretation of the result of the uncertainty analysis is difficult due to complex canopy structures [*Leuchner et al*., 2007] and the different geometric positions of the trees relative to the sun and the camera within the canopy at midday. Further research with respect to the quantification of these influences is needed. Changing fractions of different tree species over time also have to be considered.

Illumination conditions need to be quantified as a base for comparisons. Visual estimates of tree phenology for ground truthing may be hampered by the same light and visibility problems as digital camera image analysis. Weather conditions are rarely uniform and especially fog, sun angle and general brightness have a significant influence on the color sensitivity of the human eye. Considering all these aspects together, it becomes clear that, despite there is moderate uncertainty in the GF values, GF curves can be used for detection of leaf emergence dates which are typically accurate to within a few days from the validation data.

Conclusions

We found that the use of consumer-grade digital cameras offers the possibility of monitoring phenology with high temporal and spatial accuracy with respect to the phenological state of leaf emergence of individual deciduous trees. Our study clearly showed that changing illumination conditions introduce a moderate uncertainty in phenological estimates. By choosing pictures taken at a particular hour every day to monitor vegetation development, this uncertainty can be minimized. Furthermore our results suggest that species-dependant phenological observations in mixed forests are successful if overlaying signals of the different species covered by a specific analysed ROI are detected and separated. The camera should be mounted within an appropriate distance from the observed canopy to minimize scattering of the color values which aggravates automated detection of phenological transition dates.

Based on this case study for a European mixed forest we anticipate that a network of digital cameras could provide inexpensive, spatially representative and objective

460 information with the required temporal resolution for phenological applications at
461 species-level and process-based ecosystem research. In future studies the application of
462 digital camera images at sites with different dominant vegetation types such as grassland
463 sites or in agriculture should be analyzed. From a technical viewpoint, noise removal,
464 algorithm development (e.g. by optimized filtering methods) to automate the detection of
465 phenological phases, and the standardization of these algorithms for public use, should
466 receive special attention. Since these aspects are related to data processing and not to data
467 acquisition, we are convinced that phenological monitoring with digital cameras is a
468 suitable method to be used in a network of automated phenological observation sites.
469

470 **Acknowledgements**

471 This project is funded by the Federal Department of Home Affairs FDAA: State
472 Secreteriat for Education and Research SER, SBF Nr. CO5.0032. We are grateful to the
473 National Center of Competence in Research on Climate (NCCR Climate) for supporting
474 this project.

475 This publication was supported by the Foundation Marchese Francesco Medici del
476 Vascello. We acknowledge Prof. Paul Messerli for publication sponsorship.

477 We are grateful to Philipp Vock (Forestry Office, Wettingen) for field work and
478 validation data.

References

Adamsen, F. J., P. J. Pinter, E. M. Barnes, R. L. LaMorte, G. W. Wall, S. W. Leavitt, and B. A. Kimball (1999), Measuring Wheat Senescence Using a Digital Camera, *Crop Science, 39*, 719-724.

Ahl, D. E., S. T. Gower, S. N. Burrows, N. V. Shabanov, R. B. Myneni, and Y. Knyazikhin (2006), Monitoring Spring Canopy Phenology of a Deciduous Broadleaf Forest using MODIS, *Remote Sensing of Environment*, *104***,** 88-95.

Arora, V. K., and G. J. Boer (2005), A parameterization of leaf phenology for the terrestrial ecosystem component of climate models, *Global Change Biology*, *11*, 39–59.

Badeck, F. W., A. Bondeau, K. Böttcher, D. Doktor, W. Lucht, J. Schaber, and S. Sitch (2004), Responses of spring phenology to climate change, *New Phytologist, 162,* 295-309.

Baldocchi, D. D., T. A. Black, P. S. Curtis, E. Falge, J. D. Fuentas, A. Granier, L. Gu, A. Knohl, K. Pilegaard, H. P. Schmid, R. Valentini, K. Wilson, S. Wofsy, L. Xu, and S. Yamamoto (2005), Predicting the onset of net carbon uptake by deciduous forests with soil temperature and climate data: a synthesis of FLUXNET data, *International Journal of Biometeorology*, *49*(6), 377-387.

Behrens, T., and W. Diepenbrock (2006), Using Digital Image Analysis to Describe Canopies of Winter Oilseed Rape (Brassica napus L.) during Vegetative Developmental Stages, *Journal of Agronomy & Crop Science*, *192*, 295-302.

Brandhorst, A. L., and M. Pinkhof (1935), Exact determination of phyto-phenological stages, *Acte Phaenologica*, *3*, 101-109.

501 Bray, J. R., and J. E. Sanger (1961), Light reflectivity as an index of chlorophyll content
502 and production potential of various kinds of vegetation, *Proceedings of the Minnesota*
503 *Academy of Science, 29*, 222-226.
504 Bray, J. R., Sanger, J. E., and A. L. Archer (1966), The visible albedo of surfaces in
505 central Minnesota, *Ecology, 47*(4), 524-531.
506 Brügger, R., Dobbertin, M., and N. Krauchi (2003), Phenological variation of forest trees,
507 in *Phenology: An Integrative Environmental Science*, edited by M. D. Schwartz, pp.
508 255–268, Kluwer Academic Publishers, Dordrecht, Netherlands.
509 Burkard, R., P. Bützberger, and W. Eugster (2003), Vertical fogwater flux measurements
510 above an elevated forest canopy at the Lägeren research site, Switzerland, *Atmospheric*
511 *Environment*, *37*, 2979–2990.
512 Chen, J. M., and T. A. Black (1992), Defining leaf area index for non-flat leaves. *Plant,*
513 *Cell & Environment*, *15*(4), 421–429.
514 Chen, J. M., X. Li, T. Nilsonn, and A. Strahler (2000), Recent Advances in Geometrical
515 Optical Modelling and Its Applications*, Remote Sensing Reviews*, *18*, 227-2262.
516 Chuine, I., P. Yiou, N. Viovy, and B. Seguin (2004), Grape ripening as a past climate
517 indicator, *Nature*, *432*, 289-290.
518 Churkina, G., D. Schimel, B. H. Braswell, and X. Xiao (2005), Spatial analysis of
519 growing season length control over net ecosystem exchange, *Global Change Biology*,
520 *11*, 1777-1787.
521 Cleland, E. E., I. Chuine, A. Menzel, H. A. Mooney, and D. Mark (2007), Shifting plant
522 phenology in response to global change, *Trends in Ecology and Evolution, 22*(7), 357-
523 365.

524 Davis, K. J., P. S. Bakwin, C. Yi, B. W. Berger, C. Zhao, R. M. Teclaw, and J. G.
525 Isebrands (2003), The annual cycles of CO_2 and H_2O exchange over a northern mixed
526 forest as observed from a very tall tower, *Global Change Biology*, *9*, 1278-1293.
527 Dymond, J. R., and C. M. Trotter CM (1997), Directional reflectance of vegetation
528 measured by a calibrated digital camera, *Applied Optics*, *36*(18), 4314-4319.
529 Eugster, W., K. Zeyer, M. Zeeman, P. Michna, A. Zingg, N. Buchmann, and L.
530 Emmenegger (2007), Nitrous oxide net exchange in a beech dominated mixed forest in
531 Switzerland measured with a quantum cascade laser spectrometer, *Biogeosciences*
532 *Discussion*, *4*, 1167–1200.
533 Evans, G.C., and D. E. Coombe (1959), Hemispherical and woodland canopy
534 photography and the light climate, *Journal of Ecology*, *47*, 103-113.
535 Fisher, J. I., J. F. Mustard, and M. A. Vadeboncoeur (2006), Green leaf phenology at
536 Landsat resolution: Scaling from the field to the satellite, *Remote Sensing of*
537 *Environment*, *100*, 265-279.
538 Gamon, J. A., Y. Cheng, H. Claudio, L. MacKinney, and D. A. Sims (2006), A mobile
539 tram system for systematic sampling of ecosystem optical properties, *Remote Sensing of*
540 *Environment*, *103*, 246-254.
541 Graham, E., M. P. Hamilton, B. D. Mishler, P. W. Rundel, and M. H. Hansen (2006), Use
542 of a networked digital camera to estimate net CO_2 uptake of a desiccation-tolerant moss,
543 *International Journal of Plant Sciences*, *167*(4), 751-758.
544 Gu, L., W. M. Post, D. Baldocchi, T. A. Black, S. B. Verma, T. Vesala, and S. C. Wofsy
545 (2003), Phenology of vegetation photosynthesis, in *Phenology: An Integrative*

546 *Environmental Science*, edited by M. D. Schwartz, pp. 467–485, Kluwer Academic
547 Publishers, Dordrecht, Netherlands.
548 Holben, B. N. (1986), Characteristics of maximum-value composite images from
549 temporal AVHRR data, *International Journal of Remote Sensing*, *7*(11), 1417-1434.
550 Holben, B., and D. Kimes (1986), Directional reflectance response in AVHRR red and
551 near-IR bands for three cover types and varying atmospheric conditions, *Remote*
552 *Sensing of Environment*, *19*, 213-236.
553 Innes, J. L. (1994), The occurrence of flowering and fruiting on individual trees over 3
554 years and their effects on subsequent crown conditions, *Trees*, *8*, 139–150.
555 Ito, A., H. Muraoka, H. Koizumi, N. Saigusa, S. Murayama, and S. Yamamoto (2006),
556 Seasonal variation in leaf properties and ecosystem carbon budget in a cool-temperate
557 deciduous broad-leaved forest: simulation analysis at Takayama site, Japan, *Ecological*
558 *Research*, *21*, 137-149.
559 Jackson, R. D., P. M. Teillet, P. N. Slater, G. Fedosejevs, M. F. Jasinski, J. K. Aase, and
560 M. S. Moran (1990), Bidirectional measurements of surface reflectance for view angle
561 corrections of oblique imagery, *Remote Sensing of Environment*, *32*, 189-202.
562 Janeiro, F. M., F. Wagner, and A. M. Silva (2006), Visibility Measurements Using a
563 Commercial Digital Camera, paper presented at Conference on Visibility, Aerosols, and
564 Atmospheric Optics, Association for Aerosol Research, UNIQA Group Austria, Vienna,
565 Austria, 4-6 September.
566 Jonckheere, I., S. Fleck, K. Nackaerts, B. Muys, P. Coppin, M. Weiss, and F. Baret
567 (2004), Review of methods for in situ leaf area index determination Part I. Theories,

568 sensors and hemispherical photography*, Agricultural and Forest Meteorology*, *121*, 19-
569 35.
570 Kawashima, S., and M. Nakatani (1998), An Algorithm for Estimating Chlorophyll
571 Content in Leaves Using a Video Camera, *Annals of Botany*, *81*, 49-54.
572 Keeling, C. D., J. F. S. Chin, and T. P. Whorf (1996), Increased activity of northern
573 vegetation inferred from atmospheric CO_2 measurements, *Nature*, *382*, 146–149.
574 Kharin, N. G. (1976), Mathematical models in phenology, *Journal of Biogeography*, *3*,
575 357-364.
576 Kikuzawa, K. (1983), Leaf survival of woody plants in deciduous broad-leaved forests. 1.
577 Tall trees, *Canadian Journal of Botany*, *61*, 2133-2139.
578 Kikuzawa, K. (1989), Ecology and evolution of phenological pattern, leaf longevity and
579 leaf habit, *Evolutionary Trends in Plants*, *3*, 105-110.
580 Kikuzawa, K. (2003), Phenological and Morphological Adaptations to the Light
581 Environment in Two Woody and Two Herbaceous Plant Species, *Functional Ecology*,
582 *17*(1), 29-38.
583 Kira, T., and A. Kumura (1985), Dry matter production and efficiency in various types of
584 plant canopies, in: *Plant research and agroforestry,* edited by P. A. Huxley, pp. 347–
585 364, International Council for Research in Agroforestry, Nairobi, Kenia.
586 Knohl, A., E. Schulze, O. Kolle, and N. Buchmann (2003), Large carbon uptake by an
587 unmanaged 250-year-old deciduous forest in Central Germany, *Agricultural and Forest*
588 *Meteorology*, *118*, 151-167.

589 Lawrence, D. M., and J. M. Slingo (2004a), An annual cycle of vegetation in a GCM.
590 Part I: implementation and impact on evaporation, *Climate Dynamics, 22*(2 - 3), 87 -
591 105.
592 Lawrence, D.M., and J. M. Slingo (2004b), An annual cycle of vegetation in a GCM. Part
593 II: global impacts on climate and hydrology, *Climate Dynamics, 22*(2 - 3), 107 - 122.
594 Leuchner, M., A. Menzel, and H. Werner (2007), Quantifying the relationship between
595 light quality and light availability at different phenological stages within a mature mixed
596 forest, *Agricultural and Forest Meteorology*, *142*, 35–44.
597 Lieth, H. H. (1976), Contributions to phenology seasonality research, International
598 *Journal of Biometeorology*, *20*(3), 197-199.
599 Lu, L., R. A. Pielke Sr., G. Liston, W. Parton, D. Ojima, and M. Hartman (2001),
600 Implementation of a two-way interactive atmospheric and ecological model and its
601 application to the central United States, *Journal of Climate*, *14*, 900-919.
602 Menzel, A. (2002), Phenology: its importance to the global change community, *Climatic*
603 *Change*, *54*, 379–385.
604 Moore, K. E., D. R. Fitzjarrald, R. K. Sakai, M. L. Goulden, J. W. Munger, and S. C.
605 Wofsy (1996), Seasonal Variation in Radiative and Turbulent Exchange at a Deciduous
606 Forest in Central Massachusetts, *Journal of Applied Meteorology*, *35*, 122-134.
607 Morecroft, M. D., V. J. Stokes, and J. I. L. Morison (2003), Seasonal changes in the
608 photosynthetic capacity of canopy oak (Quercus robur) leaves: the impact of slow
609 development on annual carbon uptake, *International Journal of Biometeorology*, *47*,
610 221-226.

611 Niemand, C., B. Köstner, H. Prasse, T. Grünwald, and C. Bernhofer (2005), Relating tree
612 phenology with annual carbon fluxes at Tharandt forest. *Meteorologische Zeitschrift,*
613 *14*(2), 197-202.
614 Nobis, M., and U. Hunziker (2005), Automatic thresholding for hemispherical canopy-
615 photographs based on edge detection, *Agricultural and Forest Meteorology, 128*, 243-
616 250.
617 Pellika, P. (2001), Application of vertical skyward wide-angle photography and airborne
618 video data for phenological studies of beech forests in the German Alps, *International*
619 *Journal of Remote Sensing*, *22*(14), 2675-2700.
620 Peñuelas, J., and I. Filella (2001), Responses to a warming world, *Science*, *294*, 793-795.
621 Piao, S., P. Friedlingstein, P. Ciais, N. Viovy, and J. Demarty (2007), Growing Season
622 extension and its impact on terrestrial carbon cycle in the Northern Hemisphere over the
623 past 2 decades, *Global Biogeochemical Cycles*, *21*, doi:10.1029/2006GB002888.
624 Qi, J., M. S. Moran, F. Cabot, and G. Dedieu (1995), Normalization of Sun/View Angle
625 Effects Using Spectral Albedo-Based Vegetation Indices, *Remote Sensing of*
626 *Environment*, *52*, 207-217.
627 Reed, B. C., J. F. Brown, D. VanderZee, T. R. Loveland, J. W. Merchant, and D. O.
628 Ohlen (1994), Measuring Phenological Variability from Satellite Imagery, *Journal of*
629 *Vegetation Science*, *5*(5), 703-714.
630 Richardson, A. D., J. P. Jenkins, B. H. Braswell, D. Y. Hollinger, S. V. Ollinger, and M.
631 Smith (2007), Use of digital webcam images to track spring green-up in a deciduous
632 broadleaf forest. *Oecologia*, *152*, 323–334.

633 Rich, P. M. (1988), Video image analysis of hemispherical canopy photography, in: *First*
634 *Special Workshop on Videography,* edited by P. W. Mausel, pp. 84–95, American
635 Society for Photogrammetry and Remote Sensing, Terre Haute, Indiana.
636 Rich, P. M. (1990), Characterizing plant canopies with hemispherical photography, in:
637 *Instrumentation for studying vegetation canopies for remote sensing in optical and*
638 *thermal infrared regions*, *Remote Sensing Reviews*, edited by N. S. Goel and J. M.
639 Norman, *5*(1), 13–29.
640 Rich, P. M., D. B. Clark, D. A. Clark, and S. Oberbauer (1993), Long-term study of solar
641 radiation regimes in a tropical wet forest using quantum sensors and hemispherical
642 photography, *Agricultural and Forest Meteorology*, *65*, 107–127.
643 Rocha, A. V., H. B. Su, C. S. Vogel, H. P. Schmid, and P. S. Curtis (2004),
644 Photosynthetic and Water Use Efficiency Responses to Diffuse Radiation by an Aspen-
645 Dominated Northern Hardwood Forest, *Forest Science*, *50*(6), 793-801.
646 Rutishauser, T., J. Luterbacher, F. Jeanneret, C. Pfister, and H. Wanner (2007), A
647 phenology-based reconstruction of inter-annual changes in past spring seasons, *Journal*
648 *of Geophysical Research*, *112*, G04016, doi:10.1029/2006JG000382.
649 Schaaf, C. B., and A. H. Strahler (1994), Validation of bidirectional and hemispherical
650 reflectances from a geometric-optical model using ASAS imagery and Pyranometer
651 measurements of a spruce forest, *Remote Sensing of Environment*, *49*, 138-144.
652 Schulze, E. (1970), Der CO_2-Gaswechsel der Buche, *Flora*, *159*, 177-232.
653 Schwartz, M. (1994), Monitoring global change with phenology: The case of the spring
654 green wave, *International Journal of Biometeorology*, *38*(1), 18-22.

655 Sparks, T. H., K. Huber, and P. J. Croxton (2006), Plant development scores from fixed-
656 date photographs: the influence of weather variables and recorder experience,
657 *International Journal of Biometeorology*, *50*, 275-279.
658 Sparks, T. H., and A. Menzel (2002), Observed changes in seasons: an overview,
659 *International Journal of Climatology*, *22*, 1715-1725.
660 Stevens, M., C. A. Párraga, I. C. Cuthill, J. C. Partridge, and T. S. Troscianko (2007),
661 Using digital photography to study animal coloration, *Biological Journal of the Linnean*
662 *Society*, *90*, 211-237.
663 Studer, S., R. Stöckli, C. Appenzeller, and P. L. Vidale (2007), A comparative study of
664 satellite and ground-based phenology, *International Journal of Biometeorology*,
665 *51*(5), 405-414.
666 Tucker, C. J. (1979), Red and photographic infrared linear combinations for monitoring
667 vegetation, *Remote Sensing of Environment*, *8*, 127-150.
668 Vanamburg, L. K., M. J. Trlica, R. M. Hoffer, and M. A. Weltz (2006), Ground based
669 digital imagery for grassland biomass estimation, *International Journal of Remote*
670 *Sensing*, *27*(5), 939-950.
671 Wang, S., S. G. Leblanc, R. Fernandes, and J. Cihlar (2002), Diurnal variation of direct
672 and diffuse radiation and its impact on surface albedo, in *Geoscience and Remote*
673 *Sensing Symposium, IGARSS '02. 2002 IEEE International*, vol. 6, pp. 3224 – 3226.
674 White, M. A., S. W. Running, and P. E. Thornton (1999), The impact of growing-season
675 length variability on carbon assimilation and evapotranspiration over 88 years in the
676 eastern US deciduous forest, *International Journal of Biometeorology*, *42*, 139-145.

677 Zehm, A., M. Nobis, and A. Schwabe (2003), Multiparameter analysis of vertical
678 vegetation structure based on digital image processing, *Flora*, *198*, 142-160.
679 Zhang, X., M. A. Friedl, C. B. Schaaf, and A. H. Strahler (2004), Climate controls on
680 vegetation phenological patterns in northern mid- and high latitudes inferred from
681 MODIS data. *Global Change Biology, 10*, 1133-1145.
682 Zhang, X., M. A. Friedl, and C. B. Schaaf (2006), Global vegetation phenology from
683 Moderate Resolution Imaging Spectroradiometer (MODIS): Evaluation of global
684 patterns and comparison with in situ measurements, *Journal of Geophysical Research*,
685 *111,* G04017, doi:10.1029/2006JG000217.
686 Zhang, X., D. Tarpley, and J. T. Sullivan (2007), Diverse responses of vegetation
687 phenology to a warming climate, *Geophysical Research Letters*, *34*,
688 doi:10.1029/2007GL031447.
689 Zhou, Q., M. Robson, and P. Pilesji (1998), On the ground estimation of vegetation cover
690 in Australian rangelands, *International Journal of Remote Sensing*, *19*(9), 1815-1820.
691 Zhou, Q., and M. Robson (2001), Automated rangeland vegetation cover and density
692 estimation using ground digital images and a spectral-contextual classifier, *International*
693 *Journal of Remote Sensing*, *22*(17), 3457-3470.

List of Tables

List of Figures

717 tree species and dotted lines show mean unfolding dates provided by the
718 validation data.
719 Figure 3: Red and blue color fractions exemplarily for the Beech 1 ROI (a), the Ash 1
720 ROI (b) and the Background Forest ROI (c) plotted over time (day of year) for
721 2005. Solid vertical line shows start of growing season date estimated from
722 GF values.
723 Figure 4: Enlarged images of the Ash 2 ROI. Successive masking of the beech growing
724 behind the ash: (a) no leaves (April 14, 2006), (b) beech leaves unfolded (May
725 04, 2006), (c) ash masks beech (June 08, 2006).
726 Figure 5: Variation of the Green Fraction (G/(G+R+B)) during DOY 163 (June 12), 175
727 (June 24), 181 (June 30), 198 (July 17) and 211 (July 30) for each ROI.

Tables

Table 1. Regions of interest (ROI) chosen for image analysis and the main vegetation types covered by the ROI.

Region of interest	Number of pixels	Main vegetation cover
Ash 1	58696	ash, mixed background vegetation of the lower forest
Ash 2	73924	ash, beech
Ash 3	50530	ash, silver fir
Beech 1	87048	beech, ash
Beech 2	137960	beech, silver fir, understory
Beech 3	21021	beech, understory
Background Forest	61313	beech, ash, maple

744 **Table 2.** Dates for leaf unfolding in 2005 and 2006 at the Lägeren research site. Signals
745 derived from digital imagery (GF-based leaf unfolding) and validation data (visual leaf
746 unfolding) for the dominant vegetation type in each ROI are shown. Validation data is
747 based on visual image interpretation (^{V}) or based on ground observations (^{G}).

Region of interest	2005			2006		
	Visual leaf unfolding (DOY)	**GF-based leaf unfolding (DOY)**	**Absolute difference (days)**	**Visual leaf unfolding (DOY)**	**GF-based leaf unfolding (DOY)**	**Absolute difference (days)**
Ash 1	138 ^{V}	140	**2**	128 ^{V}	131	**3**
Ash 2	131 ^{V}	139	**8**	124 ^{G}	131	**7**
Ash 3	129 ^{V}	133	**4**	124 ^{V}	131	**7**
Beech 1	121 ^{V}	119	**-2**	115 ^{G}	114	**-1**
Beech 2	120 ^{V}	119	**-1**	116 ^{G}	114	**-2**
Beech 3	119 ^{V}	119	**0**	115 ^{G}	113	**-2**
Background Forest	112 ^{V}	116	**4**	111 ^{V}	114	**3**
Mean error (days)			**3**			**3.6**

748
749
750
751
752

753 **Table 3.** Mean and maximum relative change of the green fraction (GF) due to clouds in
754 2005. Results for each ROI (region of interest) are obtained by pairwise comparison of 16
755 images with different illumination conditions.

ROI	mean ΔGF [%]	max. ΔGF [%]
Ash 1	1.2	2.7
Ash 2	0.5	1.3
Ash 3	0.6	1.8
Beech 1	0.6	1.1
Beech 2	0.5	1.2
Beech 3	0.8	1.8
Background Forest	1.5	3.7

756

757 **Table 4.** GF coefficient of variation (cv) in 2006 due to changing illumination angle over
758 the day. GF variation was calculated over five sunny days in the middle and at the end of
759 the growing season.

Region of interest	DOY 163	DOY 175	DOY 181	DOY 198	DOY 211
Ash 1	1.9	1.4	1.1	1.2	1.2
Ash 2	2.0	1.5	1.2	0.4	1.1
Ash 3	2.0	1.5	1.2	0.9	0.9
Beech 1	1.7	1.4	1.0	0.6	0.9
Beech 2	1.9	1.7	1.7	1.1	1.1
Beech 3	2.8	2.5	3.0	2.0	1.8
Background Forest	2.0	1.8	1.4	0.8	1.0

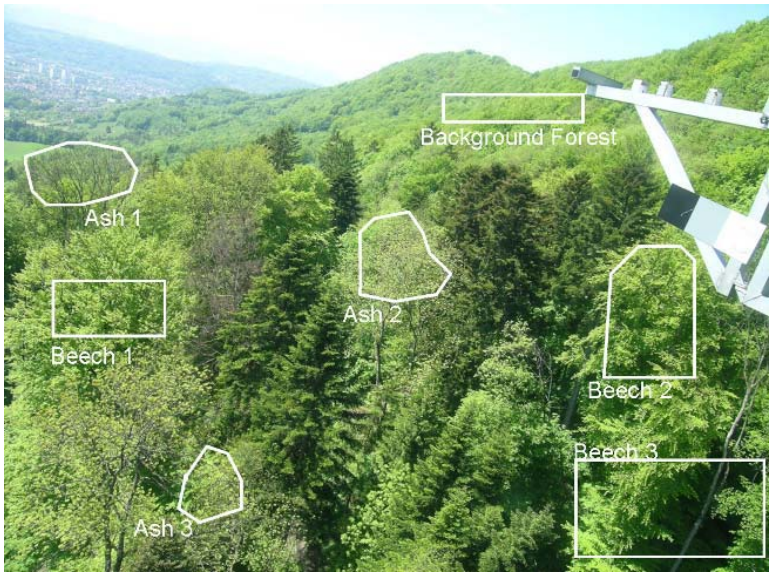

Figure 1. Sample camera image (May 24, 2005) and regions of interests (ROIs) for image analysis. A color calibration panel facing south (right) is included in all images. ROIs are named after the dominant tree sepcies.

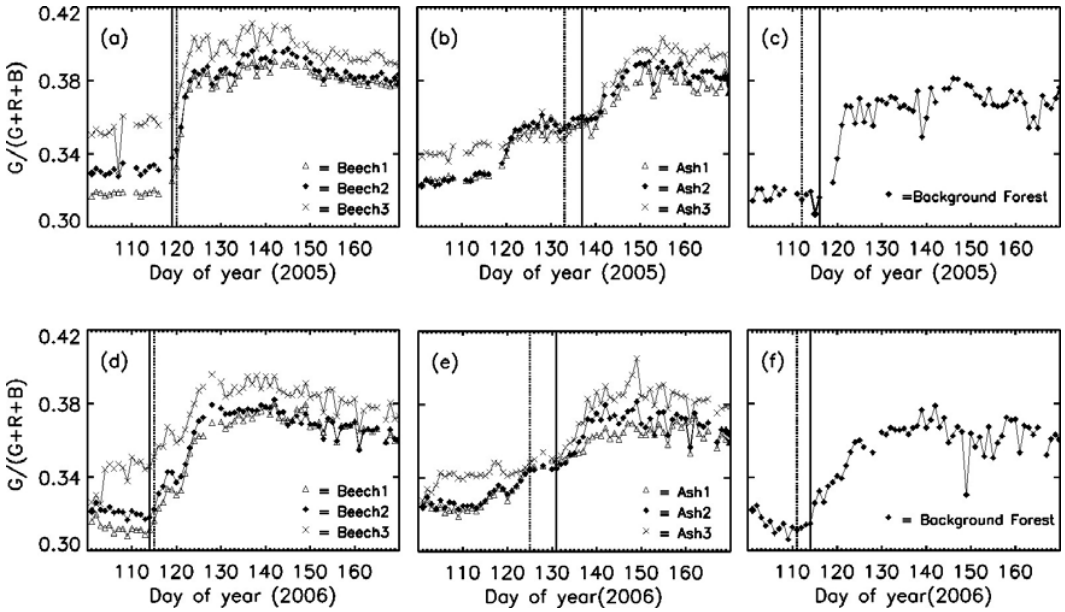

768

769 **Figure 2.** Green Fraction (G/(G+R+B)) development during spring (DOY 100-170) for

770 (a) beech-dominated ROIs in 2005 and (d) 2006, (b) ash-dominated ROIs in 2005 and (e)

771 2006 and (c) the Background Forest ROI in 2005 and (f) 2006. Solid vertical lines show

772 mean GF-based leaf unfolding dates of the dominant tree species and dotted lines show

773 mean unfolding dates provided by the validation data.

774

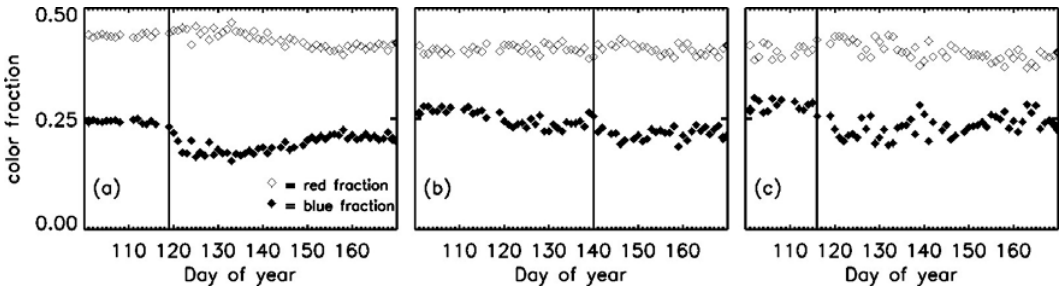

775

776 **Figure 3.** Red and blue color fractions exemplarily for the Beech 1 ROI (a), the Ash 1

777 ROI (b) and the Background Forest ROI (c) plotted over time (day of year) for 2005.

778 Solid vertical line shows start of growing season date estimated from GF values.

779

780

781

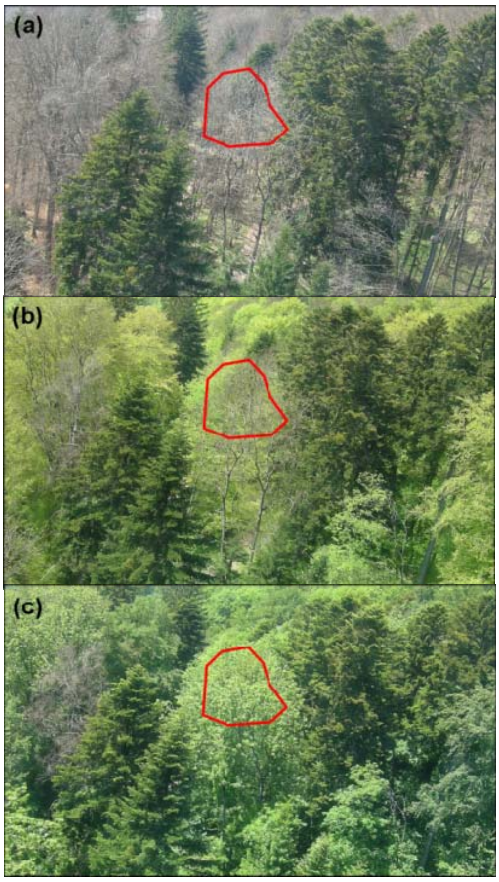

Figure 4. Enlarged images of the Ash 2 ROI. Successive masking of the beech growing behind the ash: (a) no leaves (April 14, 2006), (b) beech leaves unfolded (May 04, 2006), (c) ash masks beech (June 08, 2006).

786

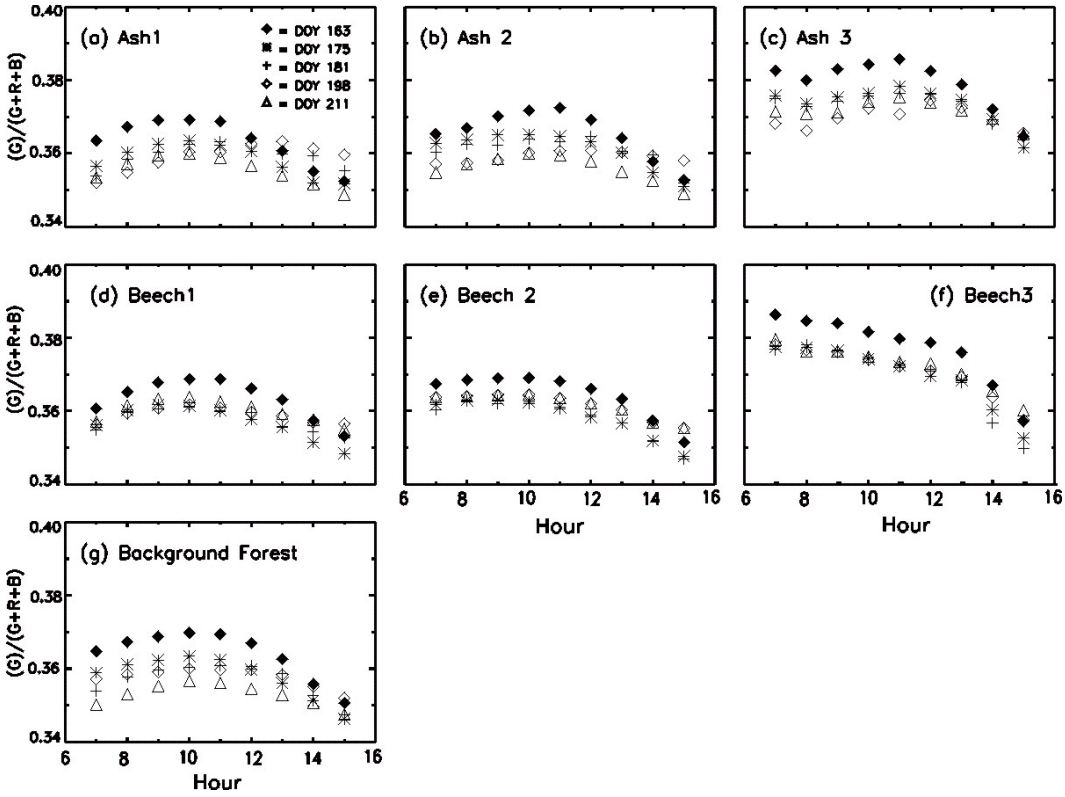

787

788 **Figure 5.** Variation of the Green Fraction (G/(G+R+B)) during DOY 163 (June 12), 175

789 (June 24), 181 (June 30), 198 (July 17) and 211 (July 30) in 2006 for each ROI.